

# Luminescence of X-ray induced radiation defects in modified lithium orthosilicate pebbles with additions of titanium dioxide

Janis Cipa<sup>1</sup>,

Gunta Kizane<sup>1</sup>,

Arnis Supe<sup>1</sup>

Aleksejs Zolotarjovs<sup>2</sup>

Arturs Zarins<sup>3</sup>

Larisa Baumanė<sup>4</sup>

<sup>1</sup> University of Latvia,  
Institute of Chemical Physics,  
1 Jelgavas street, LV-1004 Riga, Latvia  
E-mail janis.cipa@gmail.com

<sup>2</sup> University of Latvia,  
Institute of Solid State Physics,  
Department of Photonics Materials Physics,  
Laboratory of Solid State Radiation Physics,  
8 Kengaraga street, LV-1063 Riga, Latvia

<sup>3</sup> Daugavpils University,  
Faculty of Natural Science and Mathematics,  
Department of Chemistry and Geography,  
1a Parades street, LV-5401 Daugavpils, Latvia

<sup>4</sup> Latvian Institute of Organic Synthesis,  
21 Aizkraukles street, LV-1006 Riga, Latvia

Modified lithium orthosilicate ( $\text{Li}_4\text{SiO}_4$ ) pebbles with additions of titanium dioxide ( $\text{TiO}_2$ ) are designed as a possible tritium breeder ceramic for the helium cooled pebble bed (HCPB) test blanket module. Additions of  $\text{TiO}_2$  were chosen to enhance mechanical properties of the tritium breeder pebbles. The formation of radiation defects (RD) in the modified  $\text{Li}_4\text{SiO}_4$  pebbles with a different content of  $\text{TiO}_2$  was studied by X-ray induced luminescence (XRL) technique. After XRL measurements the accumulated RD were also analyzed by thermally stimulated luminescence (TSL) and electron spin resonance (ESR) spectrometry. XRL spectra consist of several bands with maxima at around 430, 490, 690, 700 and 800 nm. The XRL band with a peak at 490 nm could be associated with intrinsic defects in  $\text{Li}_4\text{SiO}_4$  matrix whereas all the other maxima at lower photon energies are the result of the addition of  $\text{TiO}_2$ .

**Keywords:** lithium orthosilicate, titanium dioxide, X-ray induced luminescence, XRL, thermally stimulated luminescence, TSL, electron spin resonance, ESR

## INTRODUCTION

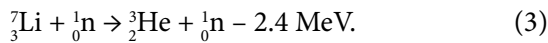
Lithium-based ceramics are suggested as a possible tritium breeder material for the helium cooled pebble bed (HCPB) test blanket module of the International Thermonuclear Experi-

mental Reactor (ITER) [1]. ITER is a large-scale scientific experiment intended to prove the viability of fusion as energy source. The easiest way to accomplish fusion reaction is the reaction between two hydrogen isotopes – deuterium ( $^2\text{D}$ ) and tritium ( $^3\text{T}$ ) (Eq. 1). The T-D fusion reaction

has a higher efficiency and probability in comparison to other reactions, such as D-D or T-T [2]:



Deuterium can be extracted from sea water, while tritium resources on Earth are very limited and thus tritium breeding is an important issue for future nuclear fusion reactors [3]. The most promising way to produce tritium is by nuclear reactions (Eqs. (2) and (3)) [4, 5]:



Modified lithium orthosilicate ( $\text{Li}_4\text{SiO}_4$ ) pebbles with additions of titanium dioxide ( $\text{TiO}_2$ ) are developed as a possible tritium breeder [6]. Due to addition of  $\text{TiO}_2$ , lithium metatitanate ( $\text{Li}_2\text{TiO}_3$ ) was obtained as a secondary phase [7]. Primarily researches show that mechanical properties of the modified  $\text{Li}_4\text{SiO}_4$  pebbles with additions of  $\text{TiO}_2$  were significantly improved compared to the reference samples –  $\text{Li}_4\text{SiO}_4$  pebbles with 10 mol% lithium metasilicate ( $\text{Li}_2\text{SiO}_3$ ) [7].

The tritium breeding ceramic during exploitation in the HCPB Test Blanket Module (TBM) will be under harsh operation conditions – neutron radiation (up to  $2.4\text{ MW m}^{-2}$  or  $10^{18}\text{ n m}^{-2}\text{ s}^{-1}$ ), high temperature (up to 1193 K), and magnetic field (up to 7–10 T) [8, 9]. Under such conditions radiation defects (RD) and radiolysis products (RP)

are induced in the tritium breeder by energetic neutrons, tritium ions, and helium ions as well as other processes. The accumulated RD and RP in the modified  $\text{Li}_4\text{SiO}_4$  pebbles could play a crucial role in the behaviour of tritium release [10]. There is evidence that RD, such as E' centres,  $\text{F}^+$  and  $\text{F}^0$  centres (oxygen vacancy trapping one or two electrons), which may form during irradiation of lithium oxide ( $\text{Li}_2\text{O}$ ),  $\text{Li}_4\text{SiO}_4$  and  $\text{Li}_2\text{TiO}_3$ , may act as effective tritium scavengers [11].

In order to evaluate the formation of RD, the modified  $\text{Li}_4\text{SiO}_4$  pebbles with a different content of  $\text{TiO}_2$  were analysed by X-ray induced luminescence (XRL) technique. After XRL measurements the samples were also analyzed by electron spin resonance (ESR) and thermally stimulated luminescence (TSL) technique.

## EXPERIMENTAL

The modified  $\text{Li}_4\text{SiO}_4$  pebbles with different contents of  $\text{TiO}_2$  were fabricated by an enhanced melt-based process at the Karlsruhe Institute of Technology (Karlsruhe, Germany) [12]. The  $\text{Li}_4\text{SiO}_4$  pebbles with 10 mol%  $\text{Li}_2\text{SiO}_3$  were selected as reference material and fabricated by a melt spraying process at SCHOTT AG (Mainz, Germany) [13]. The specifications of the investigated pebbles are shown in Table 1. The pebbles were pre-annealed in previously studied condition [7]: at 1223 K for 3 weeks in air to reduce cracks and structural defects which may form during the fabrication process.

Table 1. Specifications of the investigated  $\text{Li}_4\text{SiO}_4$  pebbles

Parameter	Sample #1	Sample #2	Sample #3	Sample #4
Phase composition	90 mol% $\text{Li}_4\text{SiO}_4$ 10 mol% $\text{Li}_2\text{TiO}_3$	80 mol% $\text{Li}_4\text{SiO}_4$ 20 mol% $\text{Li}_2\text{TiO}_3$	70 mol% $\text{Li}_4\text{SiO}_4$ 30 mol% $\text{Li}_2\text{TiO}_3$	90 mol% $\text{Li}_4\text{SiO}_4$ 10 mol% $\text{Li}_2\text{SiO}_3$
Primary component				
Li, wt%	$22.3 \pm 0.2$	$21.9 \pm 0.2$	$20.5 \pm 0.1$	$22.50 \pm 0.05$
Si, wt%	$21.4 \pm 0.05$	$18.3 \pm 0.04$	$18.5 \pm 0.1$	$24.4 \pm 0.3$
Ti, wt%	$3.99 \pm 0.02$	$8.03 \pm 0.05$	$9.55 \pm 0.01$	–
Metallic impurities				
Pt, wt%	$0.0059 \pm 0.0002$	$0.0289 \pm 0.0002$	$0.004 \pm 0.0001$	$0.0052 \pm 0.0003$
Au, wt%	<0.0004	$0.0156 \pm 0.0001$	<0.0004	<0.0004
Rh, wt%	$0.0015 \pm 0.0001$	<0.0005	$0.0017 \pm 0.0002$	<0.0005
Pebble diameter, $\mu\text{m}$	560–900	560–900	560–900	560–900

The micro-impurities of the noble metals – platinum (Pt), gold (Au), and rhodium (Rh) in the analysed samples can be explained with the corrosion of Pt alloy components, which are used both in the fabrication process [12].

For XRL measurements, the  $\text{Li}_4\text{SiO}_4$  pebbles were crushed to fine powder and pressed in  $d = 10$  mm pellets (pressure: up to 100 MPa, room temperature, air atmosphere). The optical image of the pebbles (Sample #1) and pellet is shown in Fig. 1. XRL spectra were recorded in high vacuum (lower than  $10^{-5}$  Torr) at room temperature under X-ray tube irradiation (irradiation time: 15 min, W anode, anode voltage: 40 kV, anode current: 10 mA) and recorded with the Andor Shamrock B-303i spectrograph equipped with a CCD camera (Andor Du-401A-BV) for which the XRL spectra were not corrected to compensate for the sensitivity difference of the equipment.

For ESR spectrometry, the pellets after XRL measurement were crushed into fine powder. The ESR spectra were recorded by the Bruker Biospin X-band ESR spectrometer (microwave frequency: 9.8 GHz, microwave power: 0.2 mW, modulation amplitude: 5G, field sweep: 200 and 1000 G) operating at room temperature.

The TSL glow curves of the pellets after XRL analysis were measured from 293 to 773 K (heating rate: 2 K/s, high vacuum). The TSL intensity was detected with a photomultiplier tube (HAMAMATSU H8259) with a 300–550 nm bandpass filter. To acquire information about spectral distribution of TSL, the Andor Shamrock B-303i spectrograph with a CCD camera Andor DU-401A-BV was used simultaneously with a photomultiplier tube.x

## RESULTS AND DISCUSSION

### XRL spectra of the modified $\text{Li}_4\text{SiO}_4$ pebbles with additions of $\text{TiO}_2$

The XRL spectra of the modified  $\text{Li}_4\text{SiO}_4$  pebbles with different contents of  $\text{TiO}_2$  are shown in Fig. 2. In order to understand the influence of  $\text{TiO}_2$  additions, the XRL spectrum of the reference pebbles with 10 mol%  $\text{Li}_2\text{SiO}_3$  was also included.

The formation of XRL can be divided into three main stages – the formation (i.e. ionization), thermalization, and recombination of electron-hole pairs [14]. As X-ray photons hit the sample, the electrons are removed from the valance band and excited to the conduction band, thus holes form in the valence band. The process continues as electrons either recombine emitting photons with energy close to the band gap or become trapped in defects or impurities that are already present in the sample. In the last step, trapped electrons and holes recombine and emit photons of light.

The XRL spectra of the  $\text{Li}_4\text{SiO}_4$  pebbles with 10 mol%  $\text{Li}_2\text{SiO}_3$  consist of one band with maxima at 490 nm (2.5 eV). Previously, K. Moritane et al. [15] published similar results for  $\text{Li}_2\text{SiO}_3$ ,  $\text{Li}_4\text{SiO}_4$  and  $\text{SiO}_2$  under  $\text{He}^+$  ion beam irradiation and attributed these bands to  $E'$  centers and some variants of oxygen deficiency centers (ODCs). The paramagnetic  $E'$  centre ( $\equiv\text{Si}\cdot$ ) is an unpaired electron localized in a single silicon  $\text{sp}^3$  orbital, where the “.” represents an unpaired electron and symbol “ $\equiv$ ” bands with three oxygen atoms [16]. The XRL spectra of the modified  $\text{Li}_4\text{SiO}_4$  pebbles with additions of  $\text{TiO}_2$  are



**Fig. 1.** The modified  $\text{Li}_4\text{SiO}_4$  pebbles with additions of  $\text{TiO}_2$  (Sample #1) – left, and pressed pellet – right

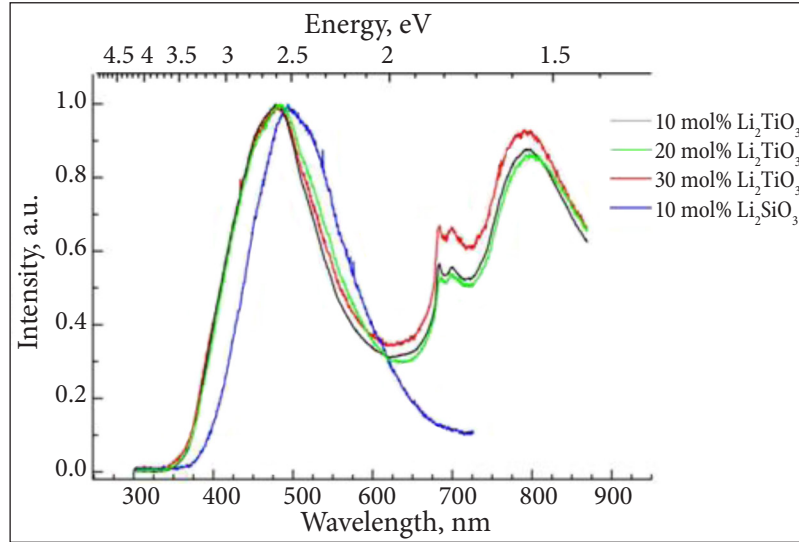


**Fig. 2.** Normalized XRL spectra of the  $\text{Li}_4\text{SiO}_4$  pebbles with different chemical composition

more complicated and contain at least five bands (Fig. 3). In order to separate these bands, the energy-based Gaussian functions were used and deconvoluted spectrum contains four main bands with wavelength 430 nm (2.9 eV), 490 nm (2.5 eV), 690 nm (1.8 eV), and 800 nm (1.55 eV). The band around 690–700 nm seems to contain two overlapped narrow peaks – 690 (1.8 eV) and 700 nm (1.77 eV). Some addition of the second order of 490 nm band is present in the red emission bands, as a diffraction grating spectrometer was used to acquire spectra. The band with wavelength 490 nm (2.5 eV) could be attributed to the primary

phase –  $\text{Li}_4\text{SiO}_4$ , while other bands might be associated with additions of  $\text{TiO}_2$ . The cathodoluminescence (CL) spectra of  $\text{Li}_2\text{TiO}_3$  were measured by V. Correcher and M. Gonzalez [17] and broad emission bands around 430, 470, and 700 nm were detected. While R. Plugaru et al. [18] detected a sharp and intense emission around 800 nm for  $\text{TiO}_2$  (at 800 nm for rutile and 820 nm for anatase).

The XRL spectra of the modified  $\text{Li}_4\text{SiO}_4$  pebbles with additions of  $\text{TiO}_2$  depending on the measurement time are shown in Fig. 4A. The obtained results show the XRL intensity decreases as irradiation time increases. As an

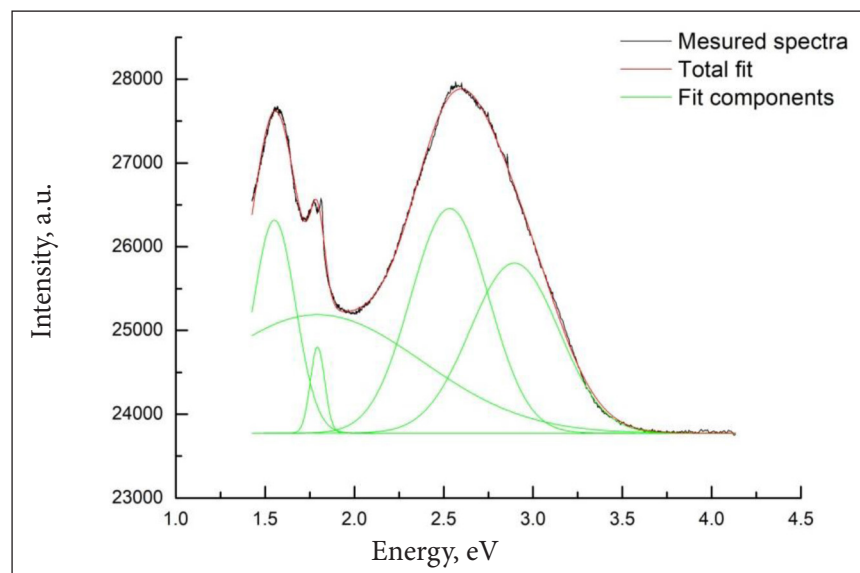


**Fig. 3.** Deconvoluted XRL spectrum of the modified  $\text{Li}_4\text{SiO}_4$  pebbles with additions of  $\text{TiO}_2$  (Sample #2)

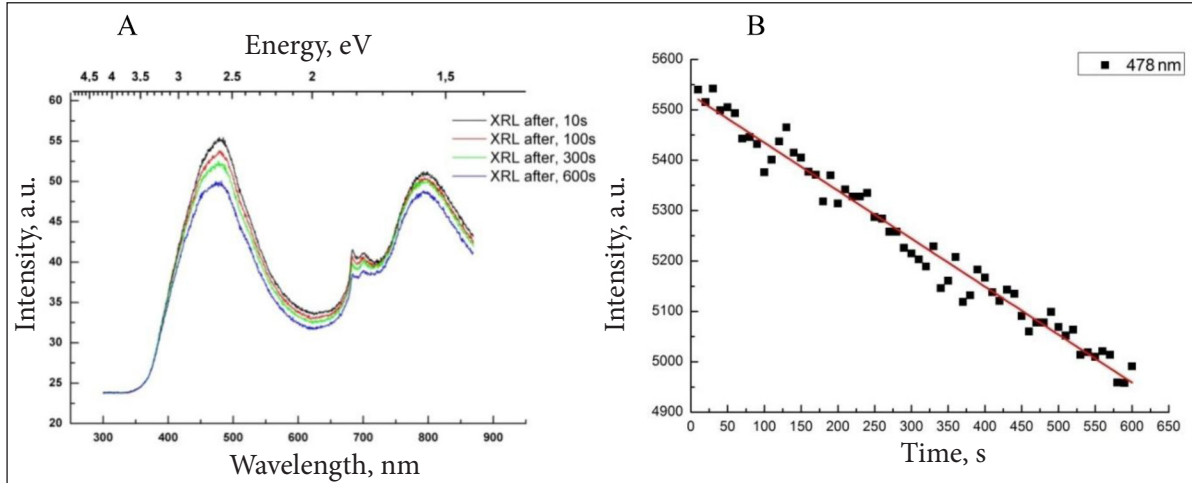


**Fig. 4.** XRL spectra of the modified  $\text{Li}_4\text{SiO}_4$  pebbles with additions of  $\text{TiO}_2$  (Sample #1) (A) and intensity of maximum with wavelength 478 nm (B) depending on irradiation

example, the intensity of the maximum with wavelength 478 nm (2.59 eV) depending on irradiation time is shown in Fig. 4B. Such decrease in intensity could be associated with the formation and recombination processes of defects present in the samples. V. Grismanovs et al. [19] reported similar effect in  $\text{Li}_2\text{O}$  and related it to oxygen vacancies introduced by annealing.

To supplement the obtained results of XRL technique and to analyse the formed electron and hole centres, the modified  $\text{Li}_4\text{SiO}_4$  pebbles with additions of  $\text{TiO}_2$  after XRL measurements were also investigated with ESR spectrometry and TSL technique.

#### ESR spectra of the modified $\text{Li}_4\text{SiO}_4$ pebbles after XRL measurements

The ESR spectra of the modified  $\text{Li}_4\text{SiO}_4$  pebbles with 10 mol%  $\text{Li}_2\text{TiO}_3$  before and after XRL measurements are shown in Fig. 5. After XRL measurements, in the ESR spectra at least three first derivative signals with  $g$ -factors  $2.019 \pm 0.001$ ,  $2.003 \pm 0.001$ , and  $1.93 \pm 0.01$  were detected. ESR technique uses quantum effects in order to detect electron spin switches as the changing magnetic field increases the energy gap for electrons under constant radiation of microwaves. There is a resonance event with a specific energy gap when

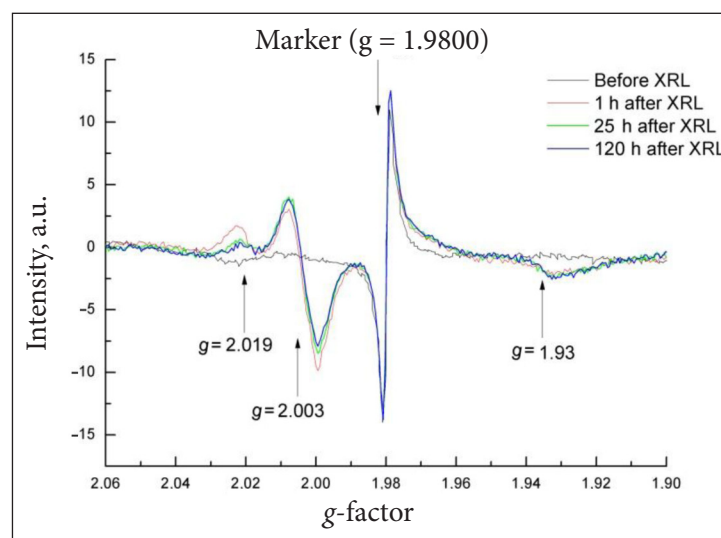


**Fig. 5.** ESR spectra of the modified  $\text{Li}_4\text{SiO}_4$  pebbles with additions of  $\text{TiO}_2$  (Sample #1) before and after XRL measurements

electrons switch the spin; thus these spectra can be observed. Dependence of resonance events on interactions inside measured material described with Zeeman and Starks effects can be used for the identification of paramagnetic RD and for better understanding of their structure.

Previously, similar ESR signals were detected and described for pure  $\text{Li}_4\text{SiO}_4$  [10],  $\text{Li}_2\text{TiO}_3$  [20], and  $\text{TiO}_2$  [21]. Therefore, the ESR signal with g-factor 2.003 most likely could be associated with  $E'$  centres ( $\text{SiO}_3^{3-}$  or  $\text{TiO}_3^{3-}$ ), and relatively small signals around 1.93 might be related to  $\text{Ti}^{3+}$  centres [22], while the unstable ESR signal at 2.019 could be associated with oxygen related defects.

#### TSL glow curves of the modified $\text{Li}_4\text{SiO}_4$ pebbles after XRL measurements

The TSL glow curve (measured with a photomultiplier tube) of the modified  $\text{Li}_4\text{SiO}_4$  pebbles with 10 mol%  $\text{Li}_2\text{TiO}_3$  after XRL measurement is shown in Fig. 6. Two major peaks at 365 and 650 K were detected. TSL measurements involve the heating of the sample and detection of emitted light from electrons and hole recombination processes. Two Gaussian peaks suggest at least

two energy depth “traps” in the pebbles with addition of  $\text{TiO}_2$ .

To acquire information about recombination centres responsible for TSL emission, the TSL spectra were measured. However, no signal was detected while measuring luminescence with a CCD camera and spectrometer. Most likely, luminescence intensity was below the detection limit of the system.

Previously, the correlation between tritium release processes and thermally annealing RD were detected [10] and thus it can be suggested that these defects could play a significant role in tritium diffusion and release behaviour. On the basis of obtained results of XRL technique, it was shown that the formation processes of RD in the modified  $\text{Li}_4\text{SiO}_4$  pebbles with additions of  $\text{TiO}_2$  slightly differ from the reference pebbles with 10 mol%  $\text{Li}_2\text{SiO}_3$ . Due to the additions of  $\text{TiO}_2$ , additional XRL bands were detected, which can be associated with  $\text{TiO}_2$  or  $\text{Li}_2\text{TiO}_3$ . To identify the formed electron and hole centres, ESR and TSL technique were used, however for precise identification of RD additional measurements need to be done. Therefore, all results also clearly confirm the necessity of further study of the radiation effects in the modified pebbles.

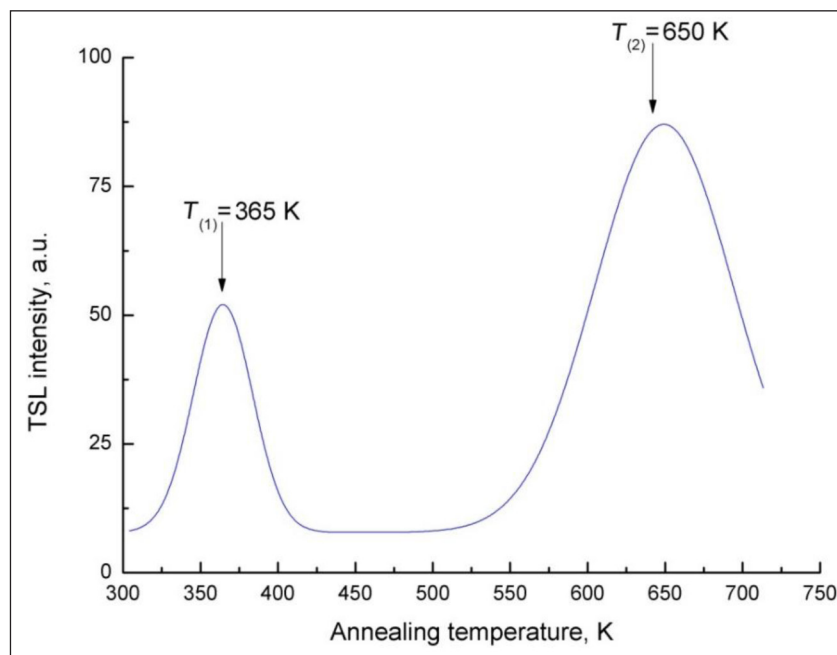


**Fig. 6.** TSL glow curve of the modified  $\text{Li}_4\text{SiO}_4$  pebbles with addition of  $\text{TiO}_2$  (Sample #1) after X-ray irradiation (15 min)



## CONCLUSIONS

In this research, the formation of radiation defects in the modified  $\text{Li}_4\text{SiO}_4$  pebbles with different contents of  $\text{TiO}_2$  was studied by XRL, ESR and TSL techniques. The obtained results of XRL indicate that a similar process occurs in the modified pebbles as in the  $\text{Li}_4\text{SiO}_4$  pebbles without addition of  $\text{TiO}_2$ . In the XRL spectra of the modified pebbles the maxima around 430 nm (2.9 eV), 490 nm (2.5 eV), 690 nm (1.8 eV), 700 nm (1.77 eV), and 800 nm (1.55 eV) were detected. Whereas in the spectra of the pebbles without addition of  $\text{TiO}_2$ , only one band with maxima at 490 nm (2.5 eV) was detected (which could be associated with intrinsic defects). Most likely, other bands are the result of the addition of  $\text{TiO}_2$ . However, additional analysis is required to identify the origins of these maxima.

In the ESR spectra of the modified pebbles, the formation of at least three first derivative ESR signals with g-factors around 1.93, 2.003, and 2.019 were detected and they were attributed to  $\text{Ti}^{3+}$  centres,  $\text{E}'$  centres, and oxygen related defects, respectively. From obtained results of TSL two peaks can be distinguished at 365 and 650 K, thus electrons are localised in traps with at least two energy levels. However, all above-mentioned results also clearly confirm the necessity in further study of the radiation induced effects in the modified mixed two-phase  $\text{Li}_4\text{SiO}_4$ - $\text{Li}_2\text{TiO}_3$  tritium breeder pebbles.

## ACKNOWLEDGEMENTS

The authors greatly acknowledge the technical and experimental support of O. Leys, M. H. H. Kolb, and R. Knitter (Karlsruhe Institute of Technology, Germany). The work is performed in the frames of the University of Latvia financed project No. Y9-B044-ZF-N-300, "Nano, Quantum Technologies, and Innovative Materials for Economics".

Received 1 March 2017

Accepted 15 May 2017

## References

- Knitter R., Chaudhuri P., Feng Y. J., Hoshino T., Yu I.-K. Recent developments of solid breeder fabrication. *Journal of Nuclear Materials*. 2013. Vol. 442. No. 1–3. P. S420–S424.
- Dorban F. Fusion energy conversation in magnetically confined plasma reactor. *Journal of Progress in Nuclear Energy*. 2012. Vol. 60. P. 89–116.
- Tanabe T. Tritium issues to be solved for establishment of a fusion reactor. *Fusion Engineering and Design*. 2012. Vol. 87. No. 5–6. P. 722–727.
- Mandal D., Sheno M. R. K., Ghosh S. K. Synthesis & fabrication of lithium-titanate pebbles for ITER breeding blanket by solid state reaction & spherodization. *Fusion Engineering and Design*. 2010. Vol. 85. No. 5. P. 819–823.
- Steiner D., Tobais M. Cross-section sensitivity of tritium breeding in a fusion reactor blanket: effects of uncertainties in cross-sections of  ${}^6\text{Li}$ ,  ${}^7\text{Li}$ , and  ${}^{93}\text{Nb}$ . *Nuclear Fusion*. 1974. Vol. 14. P. 153–163.
- Giancarli L. M. et al. Overview of the ITER TBM Program. *Fusion Engineering and Design*. 2012. Vol. 87. No. 5–6. P. 395–402.
- Knitter R. et al. Fabrication of modified lithium orthosilicate pebbles by addition of titania. *Journal of Nuclear Materials*. 2013. Vol. 442. No. 1–3. P. S433–S436.
- Vitiņš A. et al. Tritium release from breeding blanket materials in high magnetic field. *Fusion Engineering and Design*. 2007. Vol. 82. No. 15–24. P. 2341–2346.
- Boccaccini L. V. et al. Design description and performance analyses of the European HCPB test blanket system in ITER feat. *Fusion Engineering and Design*. 2002. Vol. 61–62. P. 339–344.
- Zarins A. Et al. Formation and accumulation of radiation-induced defects and radiolysis products in modified lithium orthosilicate pebbles with additions of titanium dioxide. *Journal of Nuclear Materials*. 2016. Vol. 470. P. 187–196.
- Kizane G. et al. Tritium localisation and release from the ceramic pebbles of breeder. *Journal of Nuclear Materials*. 2004. Vol. 329–333. P. 1287–1290.
- Leys O. et al. The reprocessing of advanced mixed lithium orthosilicate/metatitanate tritium breeder pebbles. *Fusion Engineering and Design*. 2016. Vol. 107. P. 70–74.
- Kolb M. H. H. et al. Enhanced fabrication process for lithium orthosilicate pebbles as breeding material. *Fusion Engineering and Design*. 2011. Vol. 86. No. 9–11. P. 2148–2151.

14. Moreira M. L. et al. Radioluminescence properties of decaoctahedral BaZrO<sub>3</sub>. *Scripta Materialia*. 2011. Vol. 64. No. 2. P. 118–121.
15. Moritani K. et al. Production behavior of irradiation defects in lithium silicates and silica under ion beam irradiation. *Journal of Nuclear Materials*. 2000. Vol. 281. No. 2–3. P. 106–111.
16. Kajihara K. <sup>18</sup>O-labeled interstitial oxygen molecules as probes to study reactions involving oxygen-related species in amorphous SiO<sub>2</sub>. *Journal of Non-Crystalline Solids*. 2012. Vol. 358. No. 24. P. 3524–3530.
17. Correcher V., Gonzalez M. On the cathodoluminescence and thermoluminescence emission of lithium titanate ceramics. *Journal of Nuclear Materials*. 2014. Vol. 445. No. 1–3. P. 149–153.
18. Plugaru R. Optical properties of nanocrystalline titanium oxide. *Thin Solid Films*. 2007. Vol. 516. No. 22. P. 179–8183.
19. Grismanovs V., Taniguchi M., Tanaka S., Yoneoka T. Study on interaction of hydrogen isotopes with radiolysis products in lithium oxide. *Journal of Nuclear Materials*. 1998. Vol. 258–263. Part 1. P. 537–542.
20. Grismanovs V., Kumada T., Tanifuji T., Nakazawa T. ESR spectroscopy of  $\gamma$ -irradiated Li<sub>2</sub>TiO<sub>3</sub> ceramics. *Radiation Physics and Chemistry*. 2000. Vol. 58. No. 2. P. 113–117.
21. Xiong L.-B., Li J.-L., Yang B., Yu Y. Ti<sup>3+</sup> in the surface of titanium dioxide: generation, properties and photocatalytic application. *Journal of Nanomaterials*. 2012. Vol. 2012. Article ID 831524. P. 1–13.
22. Lombard P., Ollier N., Boizot B. EPR study of Ti<sup>3+</sup> ions formed under beta irradiation in silicate glasses. *Journal of Non-Crystalline Solids*. 2011. Vol. 357. No. 7. P. 1685–1689.

Janis Cipa, Gunta Kizane, Arnis Supe,  
Aleksejs Zolotarjovs, Arturs Zarins, Larisa Baumanė

#### RENTGENO SPINDULIŲ SUKELTŲ DEFEKTŲ LIUMINESCENCIJA MODIFIKUOTUOSE LIČIO ORTOSILIKATO RUTULIUKUOSE SU TITANO DIOKSIDO PRIEDAIS

##### Santrauka

Modifikuoti ličio ortosilikato (Li<sub>4</sub>SiO<sub>4</sub>) rutuliukai su titano dioksido (TiO<sub>2</sub>) priedais yra suprojektuoti kaip galima tričio bryderio keramika, skirta heliu aušinamam rutuliniam įkrovos tėtiniam apvalkalo moduliui. TiO<sub>2</sub> priedai parinkti taip, kad būtų pagerintos tričio bryderio rutuliukų mechaninės savybės. Spinduliuotės defektų formavimasis modifikuotuose Li<sub>4</sub>SiO<sub>4</sub> rutuliukuose su įvairiu TiO<sub>2</sub> priedų kiekiu buvo analizuotas rentgeno spindulių sukelta liuminescencijos (XRL) technika. Atlikus XRL matavimus sukaupti spinduliuotės defektai taip pat buvo analizuoti termiškai stimuliuojama liuminescencija (TSL) ir elektronų sukimosi rezonansu (ESR). XRL spektras susideda iš keleto juostų su 430, 490, 690, 700 ir 800 nm. XRL juosta su maksimumu prie 490 nm gali būti susieta su būdingais Li<sub>4</sub>SiO<sub>4</sub> matricos defektais, kai visi kiti maksimumai su mažesne fotonų energija yra TiO<sub>2</sub> priedų įvedimo rezultatas.

**Raktažodžiai:** ličio ortosilikatas, titano dioksidas, rentgeno spindulių sukelta liuminescencija (XRL), termiškai stimuliuojama liuminescencija (TSL), elektronų sukimosi rezonansas (ESR)

Institute of Solid State Physics, University of Latvia as the Center of Excellence has received funding from the European Union's Horizon 2020 Framework Programme H2020-WIDESPREAD-01-2016-2017-TeamingPhase2 under grant agreement No. 739508, project CAMART<sup>2</sup>